2024 Carnot Liège, BE

Belgian Symposium of Thermodynamics

16-18 December 2024

University of Liège

Laboratory of Applied Thermodynamics

www.carnot2024.uliege.be

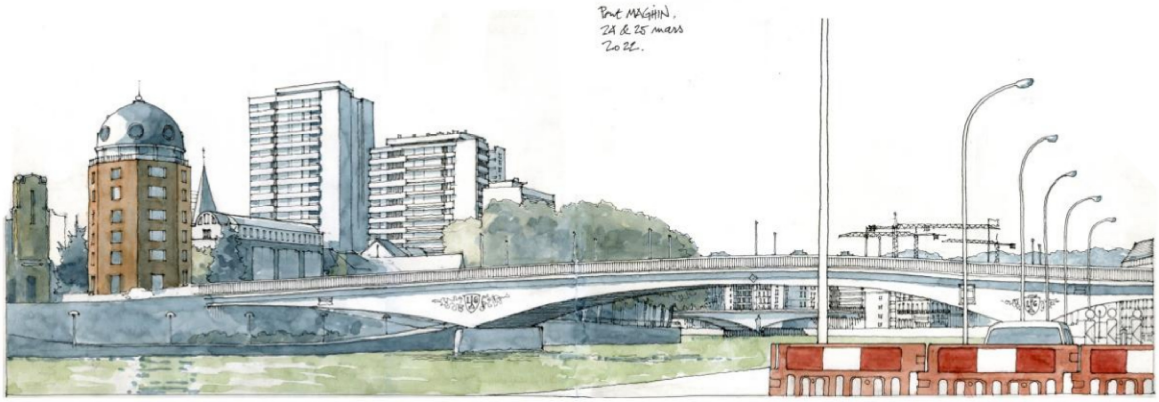

Experimental Investigation of a Supersonic Axial Impulse Turbine for a Biomass-Fired ORC CHP System

Jan Spale[1,2,*], Vaclav Vodicka[1], Philipp Streit[2,3], Vaclav Novotny[1,2], Lukas Volfl[1,2], Michal Kolovratnik[2]

[1] Czech Technical University in Prague, University Center for Energy Efficient Buildings, Energy Systems in Buildings, Bustehrad 27343, Czechia

[2] Czech Technical University in Prague, Faculty of Mechanical Engineering, Department of Energy Engineering, Prague 160 00, Czechia

[3] East Bavarian Technical University of Applied Sciences Amberg-Weiden, Centre of Excellence for Cogeneration Technologies, Amberg 92224, Germany

* *Corresponding Author: jan.spale@cvut.cz*

Abstract.

A supersonic axial impulse turbine has been developed to operate with hexamethyldisiloxane (MM) as the working fluid in a biomass-fired Organic Rankine Cycle (ORC) combined heat and power (CHP) prototype unit. The turbine is designed for a nominal electrical output of 8 kWel at a rotational speed of 18,000 rpm, with a design-point isentropic efficiency of 69 %. The design process utilized an in-house developed 1D meanline design code using genetic algorithm optimization to tune key design parameters. A hermetically sealed magnetic high-speed coupling is used to transmit power to an off-the-shelf CNC spindle, which acts as a high-speed generator. The generated power is delivered to the grid through a variable frequency drive. This paper, presented as work-in-progress, describes the turbine design, including both aerodynamic and mechanical assembly aspects. Finally, the paper presents preliminary experimental results from the field test in the biomass CHP ORC unit. Lessons learned during the initial testing phases are also highlighted, providing feedback for future improvements and optimization of small-scale ORC systems utilizing siloxane working fluids.

Keywords. Turboexpander, Organic Rankine cycle, Supersonic, Combined heat and power, Biomass, Experimental

1 Introduction and motivation

Small-scale distributed ORC systems, especially in biomass-fired setups, offer an effective way to generate both heat and electricity in a sustainable local manner. [1] However, scaling ORC technology towards a commercial product introduces unique challenges, particularly in designing efficient and cost-effective expanders, which are crucial for the system's performance and cost-effectiveness. [2]

Turbine design for small-scale ORC systems (<50 kWel) must account for the specific properties of organic fluids, such as non-ideal compressible flow behavior and high molecular complexity. [3] Traditional volumetric expanders dominate this segment due to their cost-effectiveness, off-the-shelf availability, and low sensitivity to varying thermal loads. Turbines offer an alternative with a potential for higher peak efficiencies and lower maintenance needs despite their higher initial costs and narrower operational range. [4]

This work explores the development and optimization of a supersonic axial impulse turbine using MM as the working fluid within a biomass-fired ORC CHP system. [2] The ORC unit schematics is shown below in Figure 1. The turbine design, tailored for a nominal 8 kWel output, leverages an in-house Python 1D meanline design tool optimized by a genetic algorithm to refine key design parameters. This manuscript combines aerodynamic design, mechanical considerations, and preliminary experimental results, with the goal of providing insights into performance improvements and the practical application of turbine technology in small-scale ORC systems.

2 Design methodology

The design of the supersonic axial impulse ORC turbine for the system with MM as the working fluid uses a Python 1D meanline tool. This approach uses velocity loss correlations for supersonic flow and REFPROP [5] for fluid properties and the meanline design methodology was previously reported in [3]. The lumped velocity loss correlations from turbine drives of rocket turbopumps were used. [6] These correlations were previously experimentally verified to provide reasonable results also for small-scale highly loaded ORC axial impulse turbomachinery. [4] The design was further optimized using a genetic algorithm (GA). Table 1 summarizes the cycle boundary conditions imposed to the turbine design.

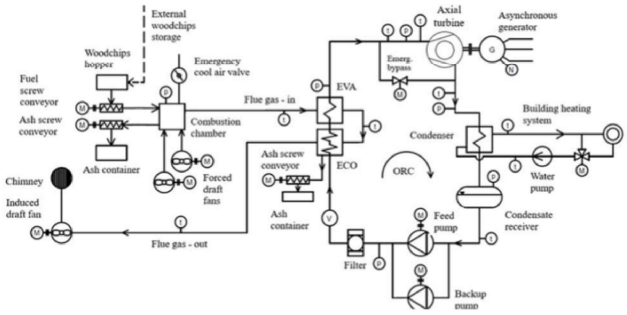

Figure 1: Piping and instrumentation diagram of the biomass-fired CHP ORC unit at CTU

The optimization routine leverages GA to refine key design parameters such as midspan diameter, blade angles, and rotational speed, aiming to maximize isentropic efficiency within the bounds of manufacturability according to Eq.(1,2). Constraints are imposed to limit flow angles and ensure feasible blade dimensions (see list below), with the goal of achieving a compact yet effective turbine layout for the target application.

- Midspan diameter (D_{mid}): 80–200 mm
- Rotational speed (n): 10,000–25,000 rpm
- Nozzle out. flow angle (α_2): 10–18°
- Blade height ratio ($\frac{h}{D_{mid}}$): 0.03–0.1
- Rotor in. flow angle (β_2): 15–30°

A tournament-selection GA (population size 80, 50 generations) was used, combining blend crossover (probability 0.5) and polynomial mutation (probability 0.2) to explore these parameter ranges systematically. For each individual, the in-house Python 1D meanline code evaluates isentropic efficiency as a global objective function under the nominal cycle boundary conditions (Table 1). The design code provides geometric and manufacturing feasibility checks.

$$f(\vec{x}) = \eta_{is}(\vec{x}); \text{ where} \quad (1)$$

$$\vec{x} = [D_{mid}, n, \alpha_s, \frac{h}{D_{mid}}, \beta_r] \quad (2)$$

Table 1: ORC boundary conditions for the turbine design

Parameter	Value	Units
Turbine inlet pressure p_{evap}	550	kPa
Turbine inlet temperature T_{in}	180	°C
Turbine inlet superheat T_{SH}	10	K
Turbine outlet pressure p_{cond}	55	kPa
Working fluid	MM	-
MM mass flow rate $\dot{m}_{wf}$	0.25	kg.s^{-1}

The aerodynamic design incorporates Method of Characteristics (MOC) for the divergent part of the supersonic nozzle design [7] using the Python *open-moc* script and a vortex-flow method [8] for the rotor profiles. Stator nozzles and rotor vanes are manufactured as prismatic blades, stator blades are de Laval nozzles and rotor blades constant channel width buckets and the rotor is shrouded to minimize tip leakage flow. Low pressure vapor exits the turbine through the diffusor to partially recover the kinetic energy at the turbine outlet. The impulse stage geometry is shown in Figure 2 in the blade-to-blade plane and the key design parameters in Table 2.

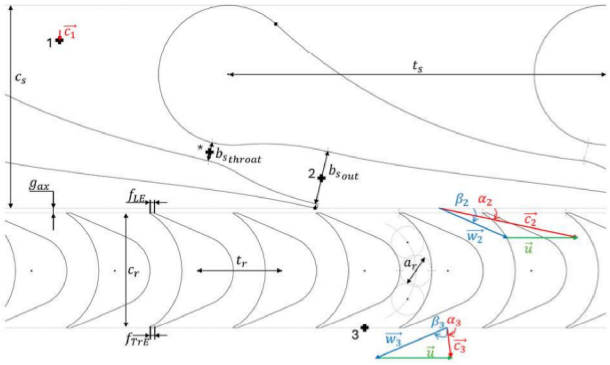

Figure 2: Cascade profile geometry in the blade-to-blade plane

Table 2: Key turbine design parameters

Parameter	Value	Units
Midspan diameter D_{mid}	135	mm
Rotational speed n	18 000	rpm
Nozzle out. Mach Ma_2	1.89	-
Nozzle out. flow angle α_2	13	°

Rotor in. flow angle β_2	23.5	°
Blade height h	5.5	mm
Number of blades Z_s, Z_r	10, 47	-
Rotor in. rel. Mach Ma_{rel2}	1.07	-
Isentropic efficiency $\eta_{is_{t-s}}$	68.1	%
Mechanical power output P_{mech}	8	kW

CFD full stage simulations using ANSYS CFX were used to validate the turbine's aerodynamic design, focusing on shockwave formation and its interactions with boundary layers, evaluating the overall performance of the turbine stage. A 3D model incorporating real-gas properties captured the non-ideal behavior of MM during vapor expansion. The CFD results informed minor adjustments to the blade profiles and clearances, helping to improve efficiency and understand the turbine flow behavior in both design and off-design conditions.

The mechanical design of the turbine assembly accounts for the high rotational speeds and includes a hermetically sealed magnetic coupling to transmit power to a high-speed generator. A water-cooled CNC spindle asynchronous motor is used as an AC high-speed generator, thus an electrical cabinet including active front end rectifier unit and a variable frequency drive is necessary for the turbine rotational speed governing and to deliver grid frequency to the local distribution network. Standard off-the-shelf shielded ball bearings greased for life with a high temperature lubricant are used. The whole turbine assembly is shown in Figure 3.

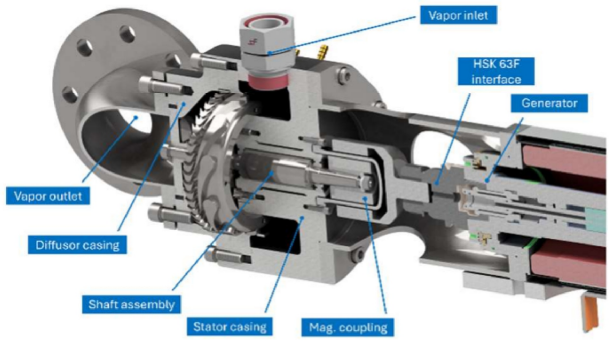

Figure 3: Cross-section view of the supersonic axial impulse turbine assembly

3 Experimental investigation

The ORC prototype unit (Figure 1) delivers heat and electricity to the CTU UCEEB research center and is used for testing various expanders. Control logic employs constant superheat PID control by varying the gear pump speed; without turbine inlet valves, the turbine inlet pressure varies with thermal input.

Due to inherently unsteady woodchips combustion, the turbine inlet pressure can fluctuate by ±10–20 kPa over a 30-minute steady-state run. The condensing pressure is fixed by the building's return water temperature (operated in CHP mode) and a 3-way valve, forcing the turbine to accommodate variable loads.

The ORC test rig uses an industrial PLC for logging and control, gathering data from the following primary sensors. Pressure transducers are ceramic capacitive elements, 0–1 MPa for high pressure, 0–400 kPa for condenser side with accuracy ±0.5 % of full scale. Temperature sensors are Pt100 resistance thermometers with accuracy ±(0.3 °C + 0.005 | T |). These are placed in thermo wells at the turbine inlet/outlet and the condenser inlet/outlet, with an overall expanded uncertainty of ±1.7 °C in the relevant 50–200 °C range with a confidence interval of 95 %. The turbine flowmeter measures volumetric flow rate of liquid MM. The range is 0–56.7 l.min^{-1} and its accuracy ±1 % of full scale. Measured liquid density is temperature and pressure-compensated via REFPROP, resulting in about 1.3 l.min^{-1} uncertainty in calculating the working fluid mass flow, the most significant source of error in the evaluation chain. Electrical power output is evaluated from the variable frequency drive (VFD) and with experimentally obtained generator efficiency curves. The combined accuracy is ±2 % of measured shaft power in the 5–10 kW range. An external handheld vibration sensor is used periodically to check shaft displacement and detect bearing anomalies. Vibration thresholds were set to ensure operation remains below ISO 10816-1 "Satisfactory" criteria. [9] These sensors enable real-time monitoring of the cycle conditions and evaluate isentropic efficiency calculations with a total uncertainty within ±2–4 percentage points, based on its absolute values.

Isentropic efficiency is calculated by comparing mechanical power output to the ideal isentropic enthalpy drop, using temperature and pressure measurements at the turbine inlet and outlet, and electrical power from the VFD with measured electric chain efficiency (Eq. (3)). An industrial PLC logs flow rates, pressures, temperatures, and electrical power for continuous monitoring and efficiency evaluation. Turbine performance was evaluated over 30-minute steady states at various pressure ratios and rotational speeds. Pressure probes measure static pressure distribution along the expansion, and a vibration meter monitors vibration intensity to prevent bearing damage.

$$\eta_{is} = \frac{P_{mech}(P_{el}, \eta_{el})}{\dot{m}_{wf}(\dot{V}_{wf}, p_{liq}, T_{liq}) \cdot \Delta h_{is}(p_{in}, p_{out}, T_{in})} \quad (3)$$

4 Preliminary results

To vary the pressure ratio (PR), the thermal input to the cycle was adjusted by changing the fuel conveyor speed (higher heat input results in pressure increase). At each pressure ratio, turbine efficiency was measured across different rotational speeds, controlled by the VFD unit via Modbus communication from the PLC. Figure 4 presents in a) the isentropic total-to-static efficiency of the turbine evaluated according to Eq.(3) and in b) turbine mechanical power output at each steady state (rpm, pressure ratio).

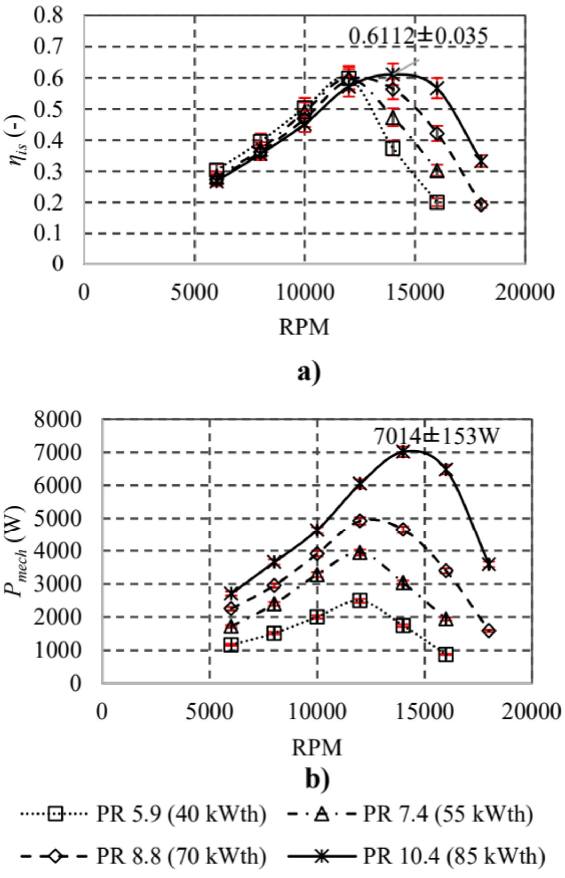

Figure 4: Experimental results of the ORC turbine test campaign, a) isentropic efficiency, b) mechanical power output

The static pressure distribution in the turbine at various points is shown in Figure 5. The nozzle works according to the design, the rotor shows a low pressure increase, probably as a result of a normal shock in the channels or the dynamic jet impinging the pressure probes tangentially at the rotor outlet, thus partially measuring the dynamic component of pressure.

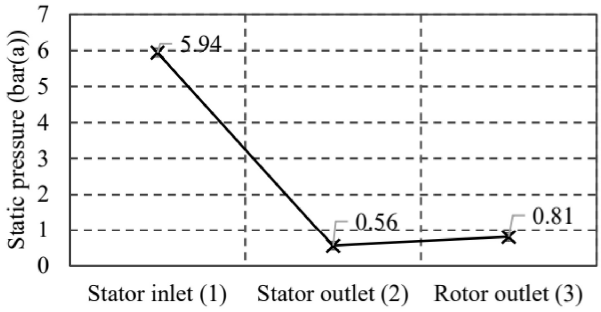

Figure 5: Static pressure along the turbine expansion at nominal pressure ratio

5 Conclusions and Future Work

This paper briefly introduces a work-in-progress in the experimental development of a small-scale supersonic axial impulse turbine for a prototype biomass-fired ORC CHP unit. The initial experimental campaigns yield the following conclusions:

- The cost-effective mechanical assembly proved reliable, showing low vibration intensity and no visible damage after 100 operational hours.
- Maximum power output (7 kW measured vs. 8 kW predicted) and isentropic efficiency (61.12 % compared to 68.1 %) was lower than modeled and occurred at a lower rotational speed (15,000 rpm vs. 18,000 rpm design), possibly due to shockwave formation at the stator trailing edge and deviations in the stator outlet flow angle.
- Measured efficiency curves are asymmetrical, with a steep decrease in power output beyond the maximum, indicating rotor choking at higher pressure ratios.
- Pressure probe measurements indicate correct operation of the supersonic nozzle at the design point but suboptimal rotor performance, suggesting normal shock choking the channels.

The future work will investigate long-term reliability under fluctuating biomass-fired ORC conditions following the building heat demand, as well as exploring advanced control strategies (VFD speed governing according to pressure ratio) to improve adaptability in small-scale CHP applications.

Acknowledgement

This material is based upon work supported by the Grant Agency of the Czech Technical University in Prague, grant No. SGS24/087/OHK2/2T/12. This work is also co-financed from the state budget by the Technology agency of the Czech Republic under the Theta Program with project no. TS01030218.

References

[1] J. Mascuch, V. Novotny, V. Vodicka, J. Spale, and Z. Zeleny, "Experimental development of a kilowatt-scale biomass fired micro – CHP unit based on ORC with rotary vane expander," *Renew. Energy*, 2018, doi: 10.1016/j.renene.2018.08.113.

[2] J. Spale, V. Vodicka, Z. Zeleny, J. Pavlicko, J. Mascuch, and V. Novotny, "Scaling up a woodchip-fired containerized CHP ORC unit toward commercialization," *Renew. Energy*, vol. 199, pp. 1226–1236, Nov. 2022, doi: 10.1016/j.renene.2022.08.144.

[3] A. P. Weiß *et al.*, "Customized ORC micro turbo-expanders - From 1D design to modular construction kit and prospects of additive manufacturing," *Energy*, p. 118407, Jul. 2020, doi: 10.1016/j.energy.2020.118407.

[4] A. P. Weiß, T. Popp, J. Müller, J. Hauer, D. Brüggemann, and M. Preißinger, "Experimental characterization and comparison of an axial and a cantilever micro-turbine for small-scale Organic Rankine Cycle," *Appl. Therm. Eng.*, vol. 140, no. January, pp. 235–244, 2018, doi: 10.1016/j.applthermaleng.2018.05.033.

[5] M. L. Huber, E. W. Lemmon, I. H. Bell, and M. O. McLinden, "The NIST REFPROP Database for Highly Accurate Properties of Industrially Important Fluids," *Ind. Eng. Chem. Res.*, vol. 61, no. 42, pp. 15449–15472, Oct. 2022, doi: 10.1021/acs.iecr.2c01427.

[6] T. W. Reynolds, "Aerodynamic Design Model II Turbine M-1 Fuel Turbopump Assembly," 1966.

[7] N. Anand, S. Vitale, M. Pini, G. J. Otero, and R. Pecnik, "Design Methodology for Supersonic Radial Vanes Operating in Nonideal Flow Conditions," *J. Eng. Gas Turbines Power*, vol. 141, no. 2, pp. 1–9, 2019, doi: 10.1115/1.4040182.

[8] L. J. Goldman and M. R. Vanco, "Computer program for design of two-dimensional sharp-edged-throat supersonic nozzle with boundary layer correction," E-6261, Aug. 1971. Accessed: Mar. 13, 2024. [Online]. Available: https://ntrs.nasa.gov/citations/19710023317

[9] "ISO 10816-1:1995(en), Mechanical vibration — Evaluation of machine vibration by measurements on non-rotating parts — Part 1: General guidelines." Accessed: Nov. 08, 2024. [Online]. Available: https://www.iso.org/obp/ui/#iso:std:iso:10816:-1:ed-1:v1:en